


Targeting stearyl-coa desaturase enhances radiation induced ferroptosis and immunogenic cell death in esophageal squamous cell carcinoma

Hui Luo, Xiaohui Wang, Shuai Song, Yunhan Wang, Qinfu Dan, and Hong Ge 

Department of Radiation Oncology, The Affiliated Cancer Hospital of Zhengzhou University, Zhengzhou, Henan, China

ABSTRACT

Overcoming resistance to radiation is a major challenge in cancer treatment. Stearyl-coa desaturase (SCD1) is the enzyme responsible for oleic acid (OA) and palmitoleic acid (POA) formation. Here, we provided evidence that targeting SCD1 was capable of inducing ferroptosis and immunogenic cell death (ICD), thereby improving the radiation sensitivity of esophageal squamous cell carcinoma (ESCC). ESCC cell lines with high SCD1 expression were treated with MF-438 (SCD1 inhibitor) to determine cell viability. Colony formation assay was performed to evaluate the radiation sensitization of SCD1 inhibitor. Tumor cell ferroptosis and ICD was analyzed in MF-438, radiation therapy (RT) and the combination treatment group. The potential molecular mechanisms underlying MF-438 as a novel radiation sensitizer in ESCC were explored. We concluded by assessing SCD1 as a prognostic factor in ESCC. MF-438 exhibited antitumor activity in ESCC cells. Our outcomes revealed significant improvement of radiation sensitivity by MF-438. Moreover, the combination treatment enhanced tumor cell ferroptosis and ICD. Further analyses revealed SCD1 conferred radiation resistance via alleviating ferroptosis in tumor cells; targeting SCD1 inhibited the biosynthesis of OA and POA, and improved radiation induced ferroptosis in ESCC cells. Clinical analysis indicated high expression of SCD1 was associated with unfavorable survival in patients of ESCC. In summary, our results demonstrated that MF-438 acted as a ferroptosis inducer. Targeting SCD1 conferred the immunogenicity of ferroptotic cancer cells and increased the effectiveness of RT in ESCC. SCD1 could be considered as a useful prognostic indicator of survival in ESCC.

ARTICLE HISTORY

Received 3 February 2022
Revised 11 July 2022
Accepted 11 July 2022

KEYWORDS



Esophageal cancer; SCD1 inhibitor; radiation therapy; ferroptosis; immunogenic cell death


Introduction

Esophageal squamous cell carcinoma (ESCC) is a complex disease that involves the transition over time from normal squamous epithelium to squamous dysplasia, and finally resulting in tumorigenesis.^{1,2} This aggressive malignancy occurs predominantly in the upper and mid-esophagus. Current evidence suggests smoking, hot drinks, dietary lack of vegetables and fruits, alcohol abuse, nitrosamines, and human papilloma virus infection are primary risk factors.^{3,4} Surgical resection, radiation therapy (RT), chemotherapy, and immunotherapy are the main antitumor strategies for ESCC.⁵ Due to atypical symptoms in the early stage, ESCC is mainly diagnosed at locally advanced or advanced stages and this may lead to iron deficiency anemia.^{2,6} RT is one of the most common treatments for inoperable, locally advanced ESCC.⁷ However, the existence of radiation resistance can result in a lack of treatment response, tumor recurrence and distant metastasis.⁸ A previous study reported the 5-year survival rate of ESCC was less than 10%, and the mechanisms governing radiation resistance were still not fully understood.²

Ferroptosis is an iron-dependent form of regulated cell death; it is novel and mainly driven by unrestricted lipid peroxidation.⁹ This type of cell death is morphologically and biologically distinct from other forms of programmed cell death, such as apoptosis.¹⁰ A previous study found that RT

was involved in a mixture of cellular events, including ferroptosis, immunogenic cell death (ICD), necrosis, mitotic catastrophe, methuosis, apoptosis, and senescence.¹¹ Ferrostatin-1 (Fer-1) is a ferroptosis inhibitor, and this compound could alleviate radiation-associated splenic lymphocytes ferroptosis by inhibiting lipid reactive oxygen species.¹² Although radiation-induced ferroptosis has been observed in cancer, tumor cells have developed diverse ferroptosis defense systems by inducing abnormal fatty acid metabolism or overexpressing key regulators of ferroptosis, such as solute carrier family 7 member 11 (SLC7A11) and glutathione peroxidase 4 (GPX4).^{13,14} Several ferroptosis-inducing strategies have been explored to eliminate cancer cell radiation resistance.^{14,15} Ye et al. demonstrated that small molecules imidazole ketone erastin (a typical ferroptosis-inducing compound, and functionally inhibits SLC7A11) and Ras Synthetic Lethal 3 (RSL3, a GPX4 inhibitor) significantly enhance radiation-induced cytoplasmic lipid peroxidation and promote clonogenic ferroptotic cell death. Moreover, the synergistic effects of radiation-mediated DNA damage and cell apoptosis were not observed upon treatment with these two compounds.¹⁶ Under metabolic stress conditions, cancer cells were able to alter lipid metabolism, resulting in ferroptosis resistance and cell survival.¹⁷ Nevertheless, the interaction between lipid metabolism and radiation-mediated ferroptosis has not yet been elucidated.

CONTACT Hong Ge  zlyygehong0199@zzu.edu.cn  Department of Radiation Oncology, The Affiliated Cancer Hospital of Zhengzhou University, Zhengzhou, Henan, China

 Supplemental data for this article can be accessed online at <https://doi.org/10.1080/2162402X.2022.2101769>

© 2022 The Author(s). Published with license by Taylor & Francis Group, LLC.

This is an Open Access article distributed under the terms of the Creative Commons Attribution-NonCommercial License (<http://creativecommons.org/licenses/by-nc/4.0/>), which permits unrestricted non-commercial use, distribution, and reproduction in any medium, provided the original work is properly cited.

Recently, Jessalyn et al. revealed that oleic acid (OA) from lymph nodes contributed to reduced ferroptosis in tumor cells.¹⁸ OA is an omega-9 fatty acid that belongs to the monounsaturated fatty acids family.¹⁹ Stearoyl-CoA desaturase (SCD1) has been described as a crucial endoplasmic reticulum enzyme responsible for converting saturated fatty acid (palmitic acid (PA) and stearic acid (SA)) to monounsaturated fatty acid (OA and palmitoleic acid (POA)).^{20,21} Impairment of lipid metabolism usually increases ferroptotic cell death.²² In several malignant tumors, SCD1 was necessary for maintain cell viability and stemness of cancer stem cells.²³ Moreover, there were a few studies demonstrating the immunogenicity of ferroptosis in which dying tumor cells promoted the maturation of immune cells.^{24,25} Therefore, we hypothesized that upregulation of SCD1 was capable of altering monounsaturated fatty acid metabolism, representing an intrinsic cytoprotective mechanism against radiation-induced ferroptosis in tumor cells.

MF-438 was initially developed as an SCD1 inhibitor that impaired the production of monounsaturated fatty acids, including OA and POA.²⁶ In the present study, we characterized the role of SCD1 in ferroptosis and demonstrated the synergistic effects of SCD1 inhibitor and RT. We also evaluated the feasibility of using SCD1 as a prognostic factor in ESCC. In addition, both a ferroptosis inducer (RSL3) and an inhibitor (Fer-1) were utilized to strengthen our conclusion.

Materials and methods

Cell cultures and reagents

ESCC cell lines were purchased from the Type Culture Collection of the Chinese Academy of Sciences. The human immortalized normal esophageal epithelial cell line SHEE was a gift from professor Liu from China-US Hormel (Henan) Cancer Institute. MF-438 (CAS: #921605-87-0) was purchased from BIOFOUNT, RSL3 (CAS: #MB4723) and Fer-1 (CAS: #MB4718) was obtained from Meilun Biotechnology. Cancer cells were maintained in RPMI 1640 medium supplied with 10% heat-inactivated fetal bovine serum (FBS) and 1% penicillin/streptomycin (100 U/ml/100ug/ml) with a humidified atmosphere at 37°C and 5% CO₂.

Western blotting

Western blot analyses were performed as described previously.²⁷ Cells were collected and lysed. The total protein concentration was determined by BCA assay (Solarbio) following the manufacturer's instruction. The proteins extracts were loaded onto a gel, separated by SDS-PAGE, and transferred to polyvinylidene difluoride (PVDF) membranes. After blocking with milk, the protein bands were incubated with diluted primary antibody and secondary antibody. Finally, the membranes were imaged with the ECL detection reagent (GE Healthcare Life Science).

Quantitative real-time PCR

Total RNA was extracted and purified from cultured primary cells using TRIzol Reagent (Invitrogen) according to the manufacturer's instruction. RNA reverse transcription was performed with the High Capacity cDNA Reverse Transcription Kit (Life Technologies) following the manufacturer's instruction. Quantitative PCR was conducted with SYBR Green PCR Master Mix using an Applied Biosystems 7500 Fast Real-Time PCR System (Life Technologies). All genes were normalized to GAPDH and exhibited as relative expression. The expression level of each gene was calculated via the $2^{-\Delta\Delta C_t}$ method. The following primers were used:

SCD 5' primer, AAACCTGGCTTGCTGATG;
 SCD 3' primer, GGGGGCTAATGTTCTTGTC A;
 GAPDH 5' primer, ATGGTGAAGGTCGGTGTGA;
 GAPDH 3' primer, AATCTCTTTGCCACTGC.

MTT assay

Tumor cells were seeded in a 96-well format with 3000 cells per well. The next morning, MF-438, RSL3 and Fer-1 were administered. Viable cells were calculated with MTT assay after 24, 48, or 72 hours. The results were measured with a microplate reader at 490 nm and expressed as the percentage of the value of control cells. Each experiment was made in triplicate.

Colony formation assay

Briefly, tumor cells were seeded 200 cells/wells and inoculated in six-well plates overnight. Then, the cells were treated with MF-438 (0.25 μ M/ml), RSL3 (0.2 μ M/ml), or Fer-1 (1 μ M/ml) for 24 hours. Next, the TrueBeam SN1403 accelerator (Varian Medical Systems) was used to deliver RT with various doses (2, 4, 6, 8, 10, 12 Gy) to cancer cells. The medium was replaced and maintained for 14 days. After stained with crystal violet, tumor colony were calculated with microscope (Olympus Corporation) and Image J software (US National Institutes of Health, Bethesda). Survival fraction were estimated using linear quadratic model as we previously reported.²⁷ All the experiments were performed 3 times.

siRNA transfection

siRNA transfection were conducted as described previously.²⁷ Generally, ESCC cells were plated in six-well format without antibiotics in the medium. The cells were grown to 40–50% confluent at the time of transfection. Transfection of siRNAs (SunYa Biotechnology, Shanghai) was performed using Lipofectamine RNAiMAX (13778150, Thermo Fisher Scientific) following the manufacturer's instructions.

Lipid peroxidation assay

C11-BODIPY581/591 is a fluorescent ratio-probe of lipid peroxidation that has been applied in the quantitation of ferroptosis.²⁸ To assess ferroptotic cell death, cells were incubated in six-well plates and treated with RT and/or indicated compounds (MF-438, RSL3, or Fer-1) for 24 hours continuous

culture. These cells were stained with 5 μ M C11-BODPY581/591 at 37°C for 30 minutes prior to trypsinization. After trypsinization and resuspension in phosphate buffered saline (PBS), lipid peroxidation was analyzed using a BD FACSCalibur Flow Cytometer (BD Biosciences).

Adenosine 5'-triphosphate (ATP) release assay

Tumor cells were seeded in six-well plates and incubated overnight. After treatment with indicated compounds and/or RT they were incubated for 6 hours. Then, the supernatants were collected and ATP was quantified using Enhanced ATP Assay Kit (#S0027, Beyotime) according to the manufacturer's instruction. LuminoskanTM Ascent (Thermo Scientific) was applied for ATP quantification, the amount of luminescence was reported as fold change in relative luminescent units (RLUs).

High mobility group protein B1 (HMGB1) release assay

Cancer cells were incubated in six-well plates. Next day, the cells were treated with indicated compounds and/or RT. After 24 hours of incubation, the supernatants were obtained for the measurement of HMGB1 concentration by Human HMGB-1 ELISA Kit (#D711210, Sangon Biotech), as described by the manufacturer. The absorbance value was measured at 450 nm using a microplate reader (Thermo Scientific).

Quantification of calreticulin on the cell surface

Briefly, tumor cells were treated with indicated compounds and/or RT and incubated for 24 hours. Then, these cells were harvested and resuspended with PBS. After fixation with 3% formaldehyde for 10 minutes at room temperature, the cells were resuspended with incubation buffer and incubated with human calreticulin antibody (#12238, CST) for 60 minutes. Next, the cells were centrifugated and resuspended in Goat Anti-Rabbit IgG H&L (Alexa Fluor[®] 488) (ab150077, Abcam) for 30 minutes. Finally, tumor cells were resuspended in cold PBS for FACS analysis.

Isolation of dendritic cells (DCs)

Peripheral blood mononuclear cells were isolated from blood of healthy donors by means of Ficoll density gradient centrifugation. Next, the EasySepTM Human CD11b positive selection Kit (STEMCELL Technologies Inc) was used to isolate macrophages. The harvested cells were then incubated in a medium supplemented with granulocyte macrophage colony-stimulating factor (500 IU/ml, Gentaur) and IL-4 (248 IU/ml, Gentaur). After 5–6 days, a population of immature DCs were obtained for cocultures with ESCC cells.

Phagocytosis assay

Tumor cells were divided into four groups including untreated control, indicated compounds, RT (6 Gy), and the combination treatment group. After treatment for 24 hours, ESCC cells were collected, washed three times and stained with CFSE (Abcam).

Then, they were washed and cocultured with immature DCs for 2 hours at ratio of 1:1. At the end of incubation, the cells were stained with mouse anti-human CD11c-phycoerythrin (PE) (BD Biosciences) or mouse IgG1-PE isotype control (BD Biosciences) for half an hour at 37°C. Phagocytosis was estimated by the Flow Cytometer (BD Biosciences). The population of double positive cells (CFSE and CD11c-PE stained cells) was calculated to obtain phagocytotic efficiency.

Survival analysis

The Gene Expression Profiling Interactive Analysis (GEPIA, <http://gepia.cancer-pku.cn>) is an online program providing multiple types of cancer and normal gene expression profiling with interactive analyses. Therefore, we applied GEPIA database to further investigate the expression and prognostic values of SCD1. The Kaplan–Meier curves were used to estimate the survival function, Hazard ratio (HR) and 95% confidence interval (95% CI) were calculated in a univariate Cox regression analysis.

In vivo tumor experiment and ethics statement

The animal experiments were approved by the Institutional Animal Care and Ethical Committee. Female severe combined immunodeficient (SCID) mice (6–8 weeks of age) were applied for animal experiment. Tumor cells suspension were subcutaneously injected into the SCID mice. After carefully monitoring until tumor burden reached to 100 mm³, mice were randomized into four groups: vehicle group (PBS), MF-438 group (MF-438 were dissolved in DMSO and subsequently diluted in PBS, orally administered at a dose of 800 μ g/kg, once a day for 2 weeks), RT group (2 Gy*5 f, once every two days), and the combined group (RT/MF-438). Mice were monitored and tumor volumes were measured two to three times per week until average volume reached to 1000 mm³; tumor volume (mm³) = (length \times width \times height \times 1/2). Then, mice were euthanized and tumors were collected. All animal care and experimental procedures were in accordance with, and were approved by the Ethics Committee of Zhengzhou University.

Statistical analysis

Statistical analysis was performed using GraphPad Prism (version 7.0, GraphPad Software). All the data were presented as means \pm standard deviation (SD). Statistical significance was calculated using student's t-tests, one-way or two-way ANOVA. The Kaplan–Meier methodology and log-rank test were applied for survival analysis. A two-tailed $p \leq .05$ was accepted as statistically significant. * $p < .05$; ** $p < .01$; *** $p < .001$; **** $p < .0001$; n.s., non-significant.

Results

SCD1 inhibitor MF-438 exerts a deleterious effect on ESCC cell viability

We first assessed the extent of SCD1 expression in seven ESCC cell lines and one normal esophageal epithelial cell line SHEE using western blot and qRT-PCR. Generally, both

intracellular levels of SCD1 protein and mRNA were broadly downregulated in normal SHEE cells when compared with ESCC cells (Figure 1a,b, supplementary Figure S1a). Among the ESCC cell lines, KYSE70 showed the highest expression of SCD1. Moreover, despite SCD1 expression being variable in multiple cell lines, there was similar trends between levels of protein and mRNA, this indicating that the elevation of SCD1 is transcriptionally driven. Since SCD1 is commonly over-expressed in ESCC cells, we hypothesized that intracellular SCD1 is essential for a wide range of cellular functions. To confirm this, we carried out cancer cell proliferation assay using MF-438, an orally bioavailable compound that inhibits SCD1 enzymatic activity. As presented in Figure 1c–i, MF-438 reduced cell viability in a dose-dependent manner in tumor cells. It was calculated that the 50% inhibitory concentration (IC50) of MF-438 in ESCC cells was between 1 and 2.4 μM . In contrast to the outcomes in tumor-derived cell lines, no deleterious effects were observed in SHEE cells treated with MF-438 (Figure 1j); 0.25 μM MF-438 is safe with minimal side effects and was utilized in the subsequent investigation.

Cell viability assays were also performed with the compounds RSL3 and Fer-1. RSL3 was able to effectively suppress cell proliferation in ESCC cells (supplementary Figure S1b–d) in a concentration-dependent manner. Both RSL3 and MF-438 were effective in inhibiting tumor cell growth. In contrast, Fer-1 was associated with no cytotoxic activity on both tumor cells and normal cells (Figure 1k–m). Altogether, these findings suggested that SCD1 inhibitor MF-438 and GPX4 inhibitor RSL3 were tumor cell-specific and potentially safe for anticancer therapy, whereas ferroptosis inhibitor Fer-1 exposure produced no cancer cell toxicity.

Targeting SCD1 boosts the effect of RT

Next, we test SCD1 inhibitor as an RT-boosting drug for ESCC treatment by colony formation assays. Both KYSE70 and KYSE410 cells were utilized in the subsequent analysis. Nontoxic concentration of MF-438 was applied prior to RT. As shown in Figure 2a,b, MF-438 significantly decreased the surviving fraction of tumor cells compared to RT alone. Notably, when cells were irradiated with a single dose of 2 Gy combined with MF-438, KYSE70 cells were much less clonogenic than KYSE410 cells. These data implied a synergistic effect between RT and SCD1 inhibitor in ESCC cells.

To further evaluated SCD1 in radiation resistance, we performed siRNA inference experiments. As presented in Figure 2c–f, knockdown of SCD1 caused minimal side effects on cell viability. In parallel with the above interpretation, knockdown of SCD1 attenuated survival fractions in both KYSE70 and KYSE410 cells when combined with RT (Figure 2g,h). In addition, we confirmed whether ferroptosis inducer works well to improve the effectiveness of RT. As expected, RSL3 significantly attenuated the surviving fraction of KYSE70 and KYSE410 cells when combined with RT (supplementary Figure S1e,f). Conversely, there was no synergistic effect between Fer-1 and RT, and pharmacological blockade of ferroptosis was even shown to increase cancer cell surviving fraction when combined with RT (Figure 2i,j).

Overall, these data clearly illustrated stimulating ferroptosis was accompanied by radiosensitization, targeting SCD1 and GPX4 were appealing strategies to sensitize ESCC cells to RT.

MF-438 induces ferroptotic cell death and synergizes with RT

With regard to SCD1 as an enzyme that catalyzes the rate-limiting step in monounsaturated fatty acid synthesis, investigators have paid attentions on alterations that occurred in lipid metabolism during ferroptosis.^{20,22} Thus, we examined whether inhibition of SCD1 causes cell death by triggering ferroptosis. As seen in Figure 3a,b, blocking SCD1 with small molecule inhibitor MF-438 induced C11-BODIPY staining in ESCC cells. This indicated that targeting SCD1 increased lipid peroxidation and caused ferroptosis, and the effect was concentration dependent. Similarly, RT mediated lipid peroxidation accumulation was detected in the current analysis (Figure 3c,d). Additionally, the combination of RT and SCD1 inhibitor resulted in a higher lipid peroxidation than RT alone in tumor cells (Figure 3c,d), indicating that reduction of SCD1 activity synergist with RT in inducing ferroptotic cell death. These results demonstrate both SCD1 inhibitor and RT were able to trigger ferroptosis in tumor cells.

We also evaluated ferroptotic cell death rates in SHEE cells. Although RT was efficient in triggering ferroptosis, the extent of lipid peroxidation in the combined group (RT/MF-438) remained similar to these in the RT group (Figure 3e,f). The outcome confirmed there was limited toxicity of MF-438 in normal cells.

Furthermore, ESCC cells treated with RSL3 showed a consistent increase of lipid peroxidation; RSL3 combined with RT exhibited synergistic effect in stimulating ferroptosis for tumor cells, but not for normal esophageal epithelial cells (supplementary Figure S2). As a negative control, Fer-1 showed a trend to attenuate the production of lipid peroxidation, and the administration of Fer-1 significantly decreased RT induced lipid peroxidation (Figure 2g–i). These outcomes strongly supported ferroptosis inducer could be utilized as a novel radiosensitizer. Taken together, our data denoted that triggering ferroptosis by targeting SCD1 and GPX4 contributed to improve the radiation sensitivity of ESCC cells.

Targeting SCD1 combined with RT triggers immunogenic ferroptosis

Immunogenic cell death (ICD) is an essential biological process during anticancer therapy.²⁹ Generally, ICD has been characterized by the translocation of calreticulin to cell surface and the release of ATP and HMGB1 into extracellular space.³⁰ ICD-associated tumor cells contributes to the activation of dendritic cells, thereby facilitating antitumor immune response. In addition to just a simple eradicating of tumor cells, radiation-induced ICD has been demonstrated in several types of tumors.^{31,32} Recently, a group explored the immunogenicity of ferroptotic cancer cells.²⁴ The induction of ferroptosis may contribute to overcome radiation resistance by improving antitumor immune response. Therefore, we examined the immunogenicity of ferroptotic cancer cells.

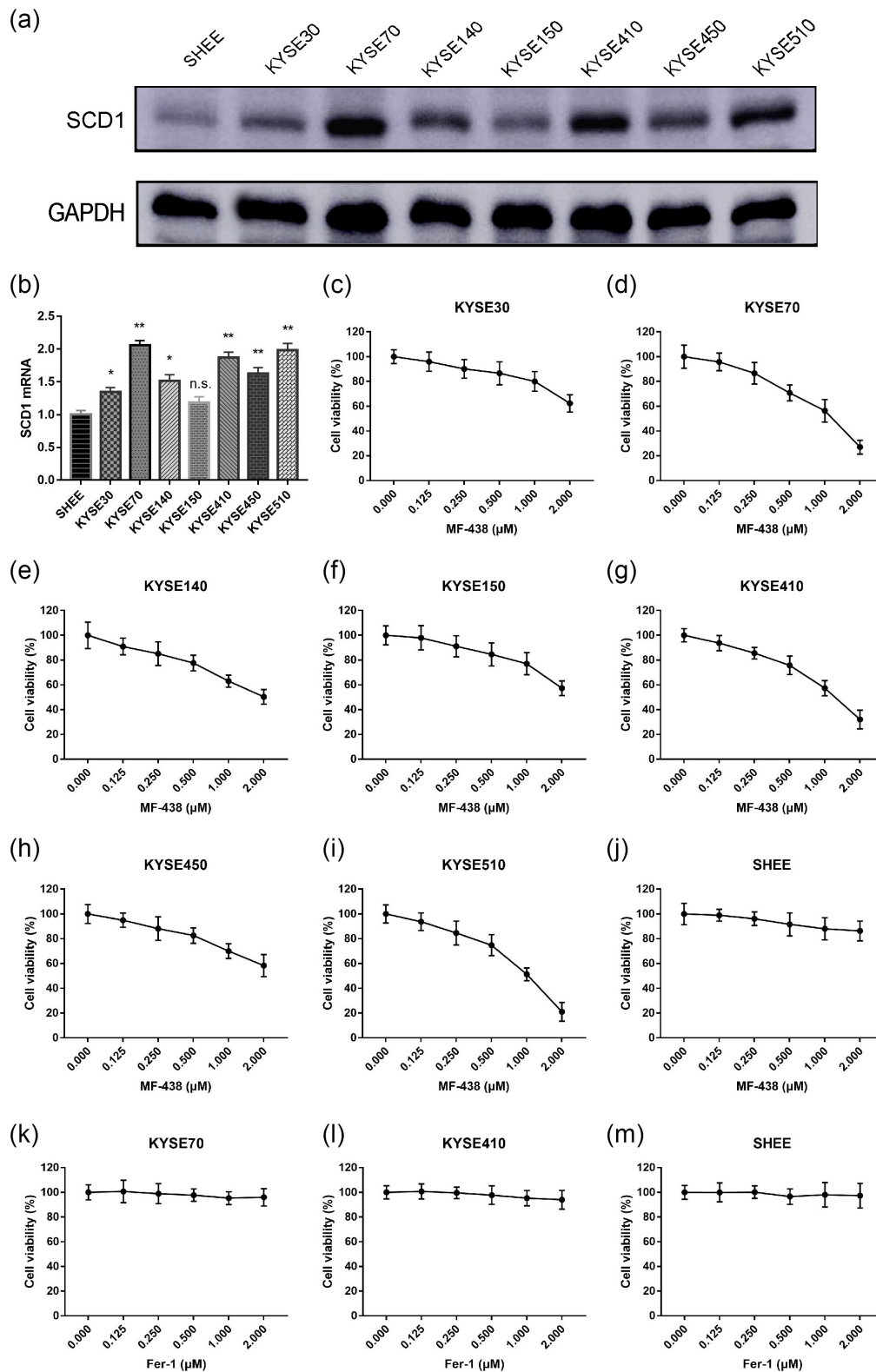


Figure 1. SCD1 protein and mRNA expression is variable across multiple cell lines, MF-438 inhibits the growth of ESCC cells. Fer-1 has minimal effect on tumor cells and normal cell. (a) The expression of SCD1 in ESCC cells and normal esophageal epithelial cells (SHEE) was analyzed by western blot. (b) Quantification of SCD1 mRNA expression in ESCC cells and SHEE cells. (c–j) Dose-survival curves of MF-438 on KYSE30, KYSE70, KYSE140, KYSE150, KYSE410, KYSE450, KYSE510 and SHEE cells were generated by MTT assay at 24 hours. (k–m) Dose-survival curves of Fer-1 on KYSE70, KYSE410, and SHEE cells and were generated by MTT assay at 24 hours. ESCC: esophageal squamous cell carcinoma; SCD1: stearyl-coa desaturase. Data are expressed as means \pm SD (n = 3), n.s., non-significant, p > .05; *p < 0.05; **p < 0.01; ***p < 0.001; ****p < 0.0001.

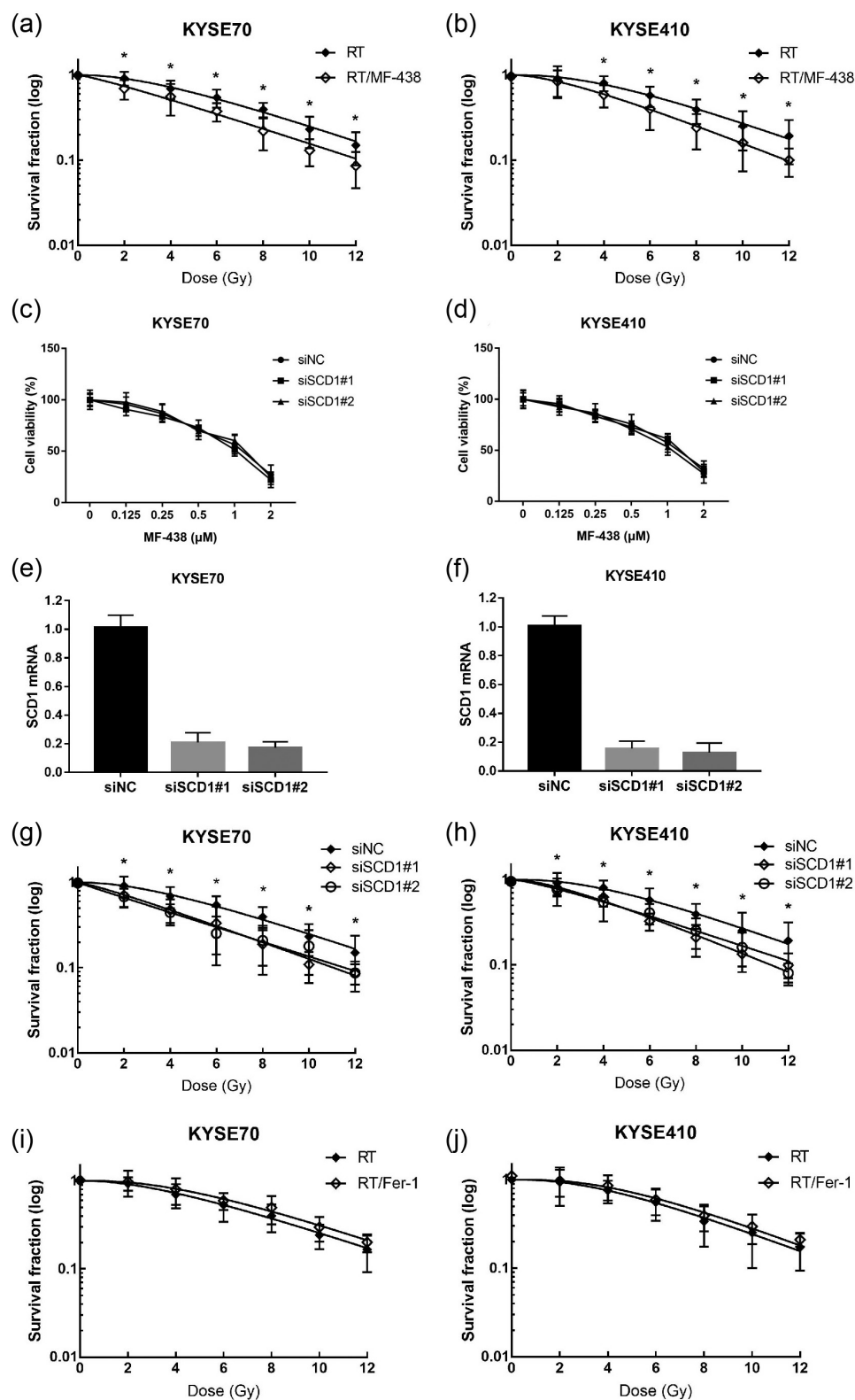


Figure 2. MF-438 enhances the radiation sensitivity of both KYSE70 cells and KYSE410 cells. Fer-1 decreases the radiation sensitivity of tumor cells. (a) Colony formation assay was performed in KYSE70 cells following RT (0, 2, 4, 6, 8, 10, and 12 Gy), or RT/MF-438 treatment (0.25 μ M). (b) Colony formation assay was performed in KYSE410 cells following RT (0, 2, 4, 6, 8, 10, and 12 Gy), or RT/MF-438 treatment (0.25 μ M). (c) Dose-survival curves of KYSE70 cells infected with siRNAs targeting SCD1 were generated by MTT assay at 24 hours. (d) Dose-survival curves of KYSE410 cells infected with siRNAs targeting SCD1 were generated by MTT assay at 24 hours. (e) qRT-PCR of KYSE70 cells infected with siRNAs targeting SCD1. (f) qRT-PCR of KYSE410 cells infected with siRNAs targeting SCD1. (g) Colony formation assay was performed in KYSE70 cells infected with siRNAs targeting SCD1. (h) Colony formation assay was performed in KYSE410 cells infected with siRNAs targeting SCD1. (i) Colony formation assay was performed in KYSE70 cells following RT (0, 2, 4, 6, 8, 10, and 12 Gy), or RT/Fer-1 treatment (1 μ M). (j) Colony formation assay was performed in KYSE410 cells following RT (0, 2, 4, 6, 8, 10, and 12 Gy), or RT/Fer-1 treatment (1 μ M). Data are expressed as means \pm SD (n = 3), n.s., non-significant, $p > .05$; * $p < 0.05$; ** $p < 0.01$; *** $p < 0.001$; **** $p < 0.0001$.

Abbreviations: RT: radiation therapy; siNC: negative control siRNA; SCD1: stearyl-coa desaturase.

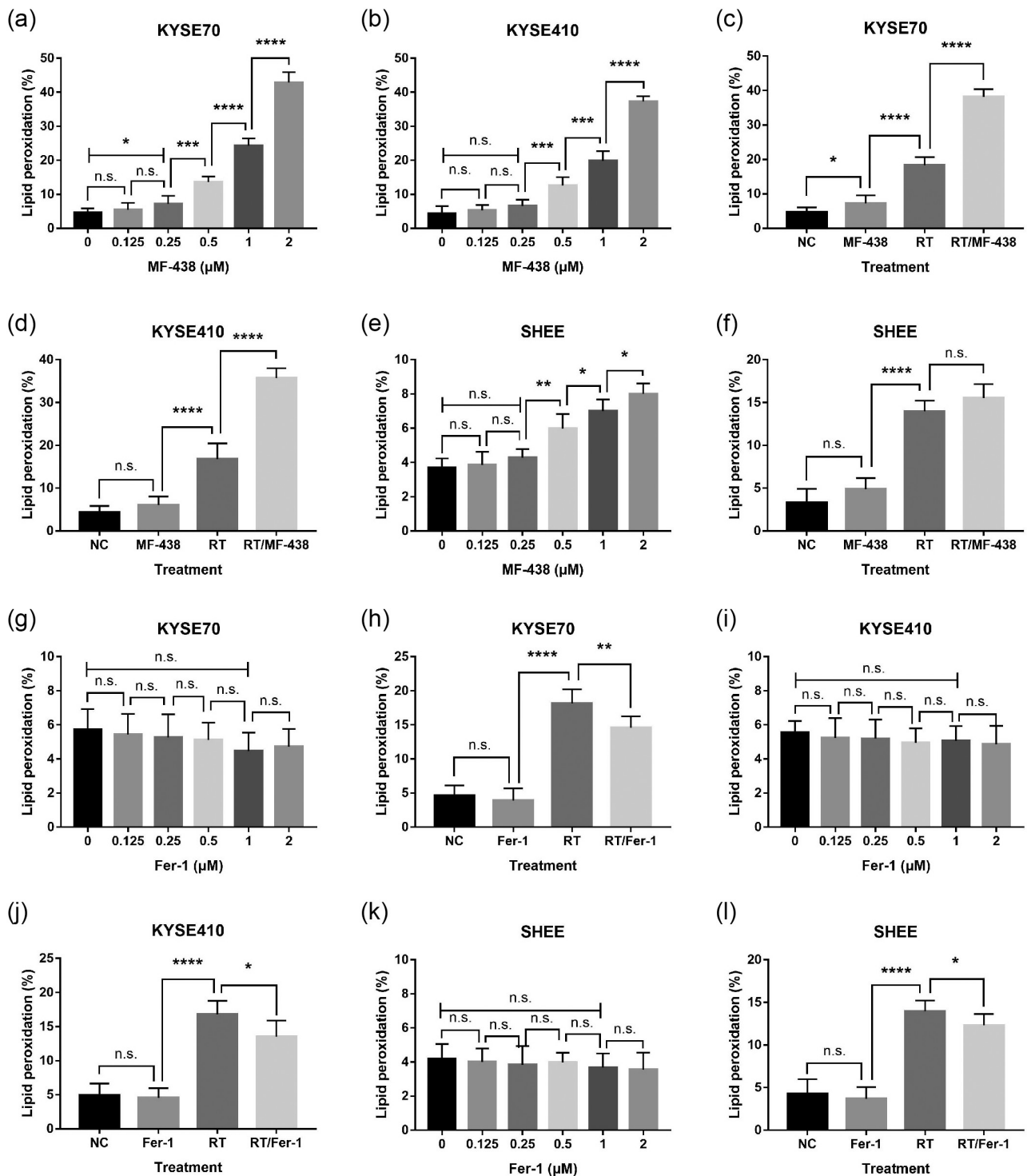


Figure 3. Targeting SCD1 was capable of inducing ferroptosis. MF-438 enhanced the efficacy of RT-induced ferroptosis in ESCC cells, while Fer-1 attenuated RT-induced ferroptosis. (a) C11-BODIPY staining was performed in KYSE70 cells following different concentrations of MF-438. (b) C11-BODIPY staining was performed in KYSE410 cells following different concentrations of MF-438. (c) C11-BODIPY staining was performed in KYSE70 cells following NC (DMSO), MF-438 (0.25 μM), RT (6 Gy), or RT/MF-438. (d) C11-BODIPY staining was conducted in KYSE410 cells following NC (DMSO), MF-438 (0.25 μM), RT (6 Gy), or RT/MF-438. (e) C11-BODIPY staining was performed in SHEE cells following different concentrations of MF-438. (f) C11-BODIPY staining was performed in SHEE cells following NC (DMSO), MF-438 (0.25 μM), RT (6 Gy), or RT/MF-438. (g) C11-BODIPY staining was performed in KYSE70 cells following different concentrations of Fer-1. (h) C11-BODIPY staining was performed in KYSE70 cells following NC (DMSO), Fer-1 (1 μM), RT (6 Gy), or RT/Fer-1. (i) C11-BODIPY staining was performed in KYSE410 cells following different concentrations of Fer-1. (j) C11-BODIPY staining was performed in KYSE410 cells following NC (DMSO), Fer-1 (1 μM), RT (6 Gy), or RT/Fer-1. (k) C11-BODIPY staining was performed in SHEE cells following different concentrations of Fer-1. (l) C11-BODIPY staining was performed in SHEE cells following NC (DMSO), Fer-1 (1 μM), RT (6 Gy), or RT/Fer-1. Data are expressed as means \pm SD ($n = 3$), n.s., non-significant, $p > .05$; * $p < 0.05$; ** $p < 0.01$; *** $p < 0.001$; **** $p < 0.0001$.

Abbreviations: ESCC: esophageal squamous cell carcinoma; NC: normal control; RT: radiation therapy; SCD1: stearyl-coa desaturase.

As shown in Figure 4a, extracellular ATP release was observed in KYSE70 cells exposed to different concentrations of MF-438; after treatment with 0.25 μM , the RLU fold increased significantly compared with untreated control group. Meanwhile, radiation-induced ATP release was detected, and correlated directly with RT dose. The combined strategies resulted in an RLU increase compared with RT alone (Figure 4b). Similar results were obtained from KYSE410 cells (Figure 4c,d). These outcomes indicated radiation-induced ATP release was enhanced by MF-438. Next, we analyzed the amount of calreticulin on the surface of cancer cells. Although MF-438 failed to induce cell-surface expression of calreticulin, RT-mediated calreticulin translocation was noticed and this effect appears to occur in a dose dependent manner (Figure 4e-h). Interestingly, there was no synergistic effect between MF-438 and RT in inducing the translocation of calreticulin to cell membrane. Finally, extracellular HMGB1

was measured among the treatment groups. Similar to the results of ATP extracellular release, both MF-438 and RT contributed to the secretion of HMGB1 from tumor cells to extracellular space. The combination of RT and MF-438 resulted in enhanced HMGB1 extracellular release (Figure 4i-l).

To validate the role of ferroptosis in mediating ICD, tumor cells were incubated with both RSL3 and Fer-1. For a positive control, we noted the generation of both ATP and HMGB1 in extracellular milieu after treatment with ferroptosis inducer RSL3 and there was a synergistic effect between RSL3 and RT. Consistent with the MF-438 data, RSL3 had no effect on the translocation of calreticulin to the cell membrane (supplementary Figure S3a-m). In the meantime, RT-induced ATP and HMGB1 release could be attenuated by ferroptosis inhibitor Fer-1, and we were unable to detect an alteration of the exposure of calreticulin to the cell surface (supplementary Figure S4). Importantly,

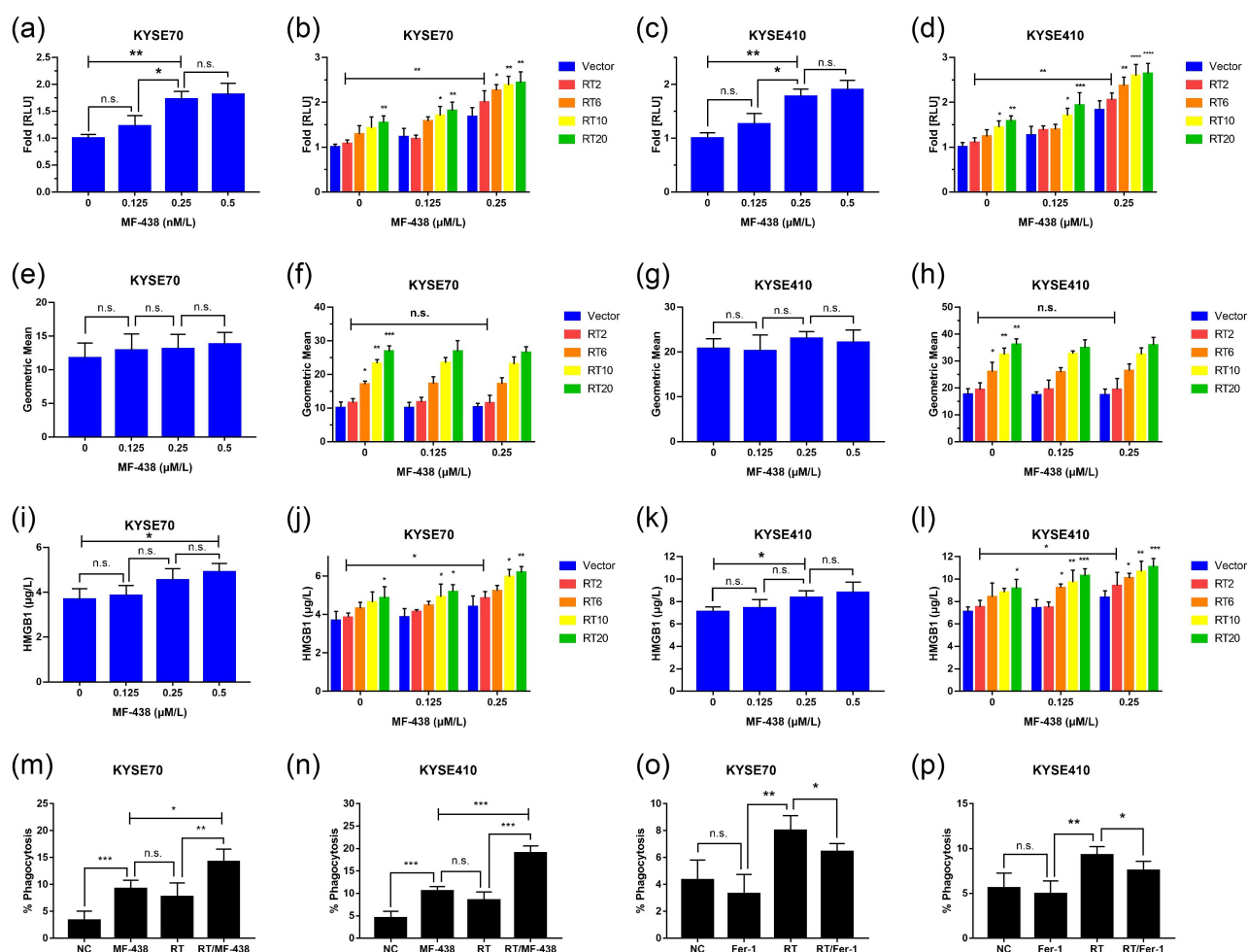


Figure 4. Targeting SCD1 combined with RT triggers immunogenic ferroptosis. Suppressing ferroptosis attenuates the uptake of cancer cells by DCs. (a) Extracellular ATP release in KYSE70 cells following different concentrations of MF-438. (b) RT combined with MF-438 resulted in enhanced extracellular ATP release in KYSE70 cells. (c) Extracellular ATP release in KYSE410 cells following different concentrations of MF-438. (d) RT combined with MF-438 resulted in enhanced extracellular ATP release in KYSE410 cells. (e) Calreticulin cell surface exposure in KYSE70 cells following different concentrations of MF-438. (f) Calreticulin cell surface exposure in KYSE70 cells following different doses of RT combined with MF-438. (g) Calreticulin cell surface exposure in KYSE410 cells following different concentrations of MF-438. (h) Calreticulin cell surface exposure in KYSE410 cells following different doses of RT combined with MF-438. (i) Extracellular HMGB1 release in KYSE70 cells following different concentrations of MF-438. (j) RT combined with MF-438 resulted in enhanced extracellular HMGB1 release in KYSE70 cells. (k) Extracellular HMGB1 release in KYSE410 cells following different concentrations of MF-438. (l) RT combined with MF-438 resulted in enhanced extracellular HMGB1 release in KYSE410 cells. (m-n) The uptake of ferroptotic cells by DCs after treated with MF-438, RT, or the combined regimen. (o-p) The uptake of ferroptotic cells by DCs after treated with Fer-1, RT, or the combined regimen. Data are expressed as means \pm SD ($n = 3$), n.s., non-significant, $p > .05$; * $p < 0.05$; ** $p < 0.01$; *** $p < 0.001$; **** $p < 0.0001$.

Abbreviations: ATP: adenosine triphosphate; DCs: dendritic cells; HMGB1: High mobility group box protein 1; RT: radiation therapy; SCD1: stearoyl-coa desaturase.

ferroptosis was accompanied by extracellular release of ATP and HMGB1, also known as immunogenic ferroptosis. MF-438, in combination with RT, was highly efficient in triggering ICD.

MF-438 and RT combined resulted in enhanced DC phagocytosis of dying tumor cells

Afterward, we sought to identify whether immunogenic ferroptosis could facilitate cancer cell recognition and phagocytosis by DCs. As illustrated in Figure 4m,n, ESCC cells were efficiently phagocytosed by DCs within a few hours after the administration of MF-438; compared with RT alone, a higher phagocytotic efficiency was observed when tumor cells were treated with the combined regimen. Moreover, RSL3 seems much more efficient than MF-438 in assisting phagocytosis of ESCC cells by DCs (supplementary Figure S3n–p). For a negative control, we inhibited immunogenic ferroptosis by treating ESCC cells with Fer-1. Inhibiting ferroptosis significantly reduced radiation-mediated phagocytic clearance (Figure 4o,p). Hence, the results suggest that the immunogenic ferroptosis-associated dying tumor cells were recognized and phagocytosed efficiently by the DCs, causing DC activation.

MF-438 induces ferroptosis through decreasing the formation of monounsaturated fatty acids

It is well-known that SCD1 is involved in lipid remodeling and inhibition of SCD1 leads to decreased production of monounsaturated fatty acids – OA and POA.^{20,21} Thus, we focused on the role of lipid metabolism in regulating ferroptosis. Phospholipids containing polyunsaturated fatty acids were the type of lipids that are distinctly susceptible to peroxidation.³³ In addition to reactive oxygen species accumulation, RT is also involved in lipid metabolism and contributed to the biosynthesis of phospholipids containing polyunsaturated fatty acids. Altogether, RT can lead to lipid peroxidation and promotion of ferroptosis.^{34,35} Monounsaturated fatty acids, including OA and POA, have been described to suppress ferroptosis in cells.^{18, 28} Therefore, we hypothesized that SCD1-mediated monounsaturated fatty acids synthesis played an essential role in radiation resistance by reducing ferroptosis.

As shown in Figure 5a–d, ferroptotic cell death triggered by RT exposure could be recapitulated with exogenous OA or POA, two monounsaturated fatty acids formed by SCD1 activation. Conversely, RT-induced ferroptosis could not be rescued by PA (Figure 5e,f) or SA (Figure 5g,h), the two corresponding saturated fatty acids. Similarly, tumor cells exposed to either OA or POA showed increased radiation resistance (Figure 5i–l) and this effect was not detected after cancer cells incubated with PA or SA (supplementary Figure S5a–d). Collectively, SCD1 was a crucial component that participates in lipid peroxidation as both OA and POA conferred treatment resistance by alleviating radiation-induced ferroptosis. MF-438 decreased OA and POA synthesis and acted as a novel radiosensitizer that weakened cancer cells by inducing lipid peroxidation.

MF-438 sensitizes tumor cells to RT and suppress ESCC growth in vivo

Given all the above data, we decided to investigate the therapeutic potential of SCD1 inhibitor combined with RT *in vivo*. Mice with subcutaneous ESCC tumors were treated with either vehicle alone, MF-438 alone, RT alone, or the combination of RT and MF-438. Untreated control mice or MF-438 treated mice rapidly developed noticeable tumor growth throughout the analysis (Figure 6a,b). Conversely, treatment of mice with RT led to a dramatically stronger suppression of tumor growth than those from the untreated control or MF-438 treated mice. Remarkably, mice that received combination therapy resulted in the most extensive tumor shrinkage compared with untreated control, MF-438, or RT-treated mice (supplementary Figure S5e). Furthermore, there was no apparent toxicity in mice treated with MF-438 (Figure 6c). Together with, these findings clearly demonstrated the antitumor activity of MF-438 *in vivo* and revealed that the compound can be exploited to enhance radiation response in the treatment of ESCC.

Overexpression of SCD1 in ESCC is correlated with unfavorable survival

As consistently demonstrated in the study, SCD1 activity confers radiation resistant in tumor cells. To clarify and distinguish the role of SCD1 in patients with ESCC, we next investigated GEPIA database according to gene-expression profile. ESCC patients were divided into two groups based on the levels of SCD expression: high and low. High SCD expression was associated with shorter disease-free survival in patients of ESCC compared with low SCD expression group (17.9 months versus 26.7 months, $P = .025$; Figure 6d). In addition, SCD was significantly upregulated in tumor tissues compared with normal epithelium in esophagus (Figure 6e). These observations were consistent with the outcomes from cell lines. Accordingly, our results strongly suggest that SCD expression could be a useful biomarker to identify subsets of ESCC that would be sensitive or resistant to this combination treatment.

Discussion

Over the last few years, it is noteworthy that the successive discovery and ongoing study of ferroptosis have shown it to be a promising form of non-apoptotic cell death in the development of innovative cancer therapies.^{9,10} In the present analysis, we characterized the variable expression of SCD1 in multiple ESCC cell lines and a normal esophageal epithelial cell line. OA and POA, two products of SCD1 activity, conferred radiation resistance in tumor cells by reducing accumulation of lipid peroxidation. Consistently, targeting SCD1 caused immunogenic ferroptosis and improved the efficacy of RT. Meanwhile, radiation-induced ferroptosis and ICD were also observed in our study. Additionally, our data revealed SCD1 as a prognostic factor for survival in patients of ESCC, with higher expression of SCD1 being associated with poor survival.

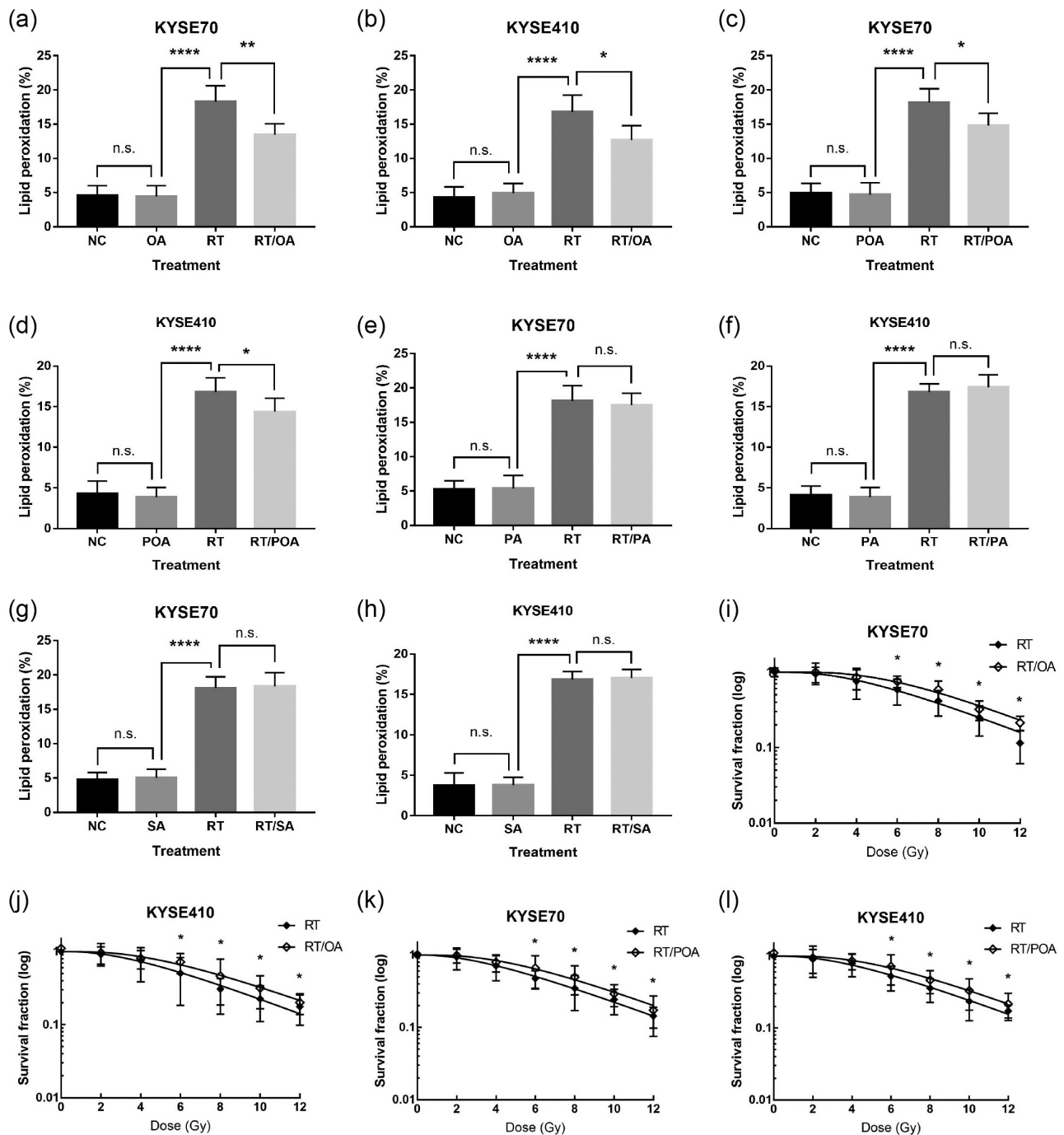


Figure 5. Monounsaturated fatty acids (OA and POA) protect tumor cells from radiation-induced ferroptosis and lead to radiation resistance. However, RT-induced lipid peroxidation could not be mitigated by saturated fatty acids (PA and SA). (a) C11-BODIPY staining analyzed by flow cytometry in KYSE70 cells following NC (DMSO), OA (0.1 mM), RT (6 Gy), or RT/OA. (b) C11-BODIPY staining analyzed by flow cytometry in KYSE410 cells following NC (DMSO), OA (0.1 mM), RT (6 Gy), or RT/OA. (c) C11-BODIPY staining analyzed by flow cytometry in KYSE70 cells following NC (DMSO), POA (0.1 mM), RT (6 Gy), or RT/POA. (d) C11-BODIPY staining analyzed by flow cytometry in KYSE410 cells following NC (DMSO), POA (0.1 mM), RT (6 Gy), or RT/POA. (e) C11-BODIPY staining analyzed by flow cytometry in KYSE70 cells following NC (DMSO), PA (0.1 mM), RT (6 Gy), or RT/PA. (f) C11-BODIPY staining analyzed by flow cytometry in KYSE410 cells following NC (DMSO), PA (0.1 mM), RT (6 Gy), or RT/PA. (g) C11-BODIPY staining analyzed by flow cytometry in KYSE70 cells following NC (DMSO), SA (0.1 mM), RT (6 Gy), or RT/SA. (h) C11-BODIPY staining analyzed by flow cytometry in KYSE410 cells following NC (DMSO), SA (0.1 mM), RT (6 Gy), or RT/SA. (i-j) Colony formation assay was performed in tumor cells following RT (0, 2, 4, 6, 8, 10, and 12 Gy), or RT/OA treatment (0.1 mM). (k-l) Colony formation assay was performed in cancer cells following RT (0, 2, 4, 6, 8, 10, and 12 Gy), or RT/POA treatment (0.1 mM). Data are expressed as means \pm SD ($n = 3$), $p > .05$; * $p < 0.05$; ** $p < 0.01$; *** $p < 0.001$; **** $p < 0.0001$.

Abbreviations: NC, normal control; OA, oleic acid; PA, palmitic acid; POA, palmitoleic acid; RT, radiation therapy; SA, stearic acid; SCD1, stearoyl-coa desaturase; n.s, non-significant.

Lipids are essential regulators of various cellular processes, and lipid metabolism is involved in regulated cell death.³⁶ It has been shown that the extensive lipid peroxidation of phospholipids in the cell membrane is a prerequisite to

ferroptosis.¹⁴ Previous analysis showed that inhibiting SCD1 disturbed intracellular lipid homeostasis and induced ferroptosis in tumor cells.²⁶ The two monounsaturated fatty acids OA and POA have been reported to protect tumor cells from

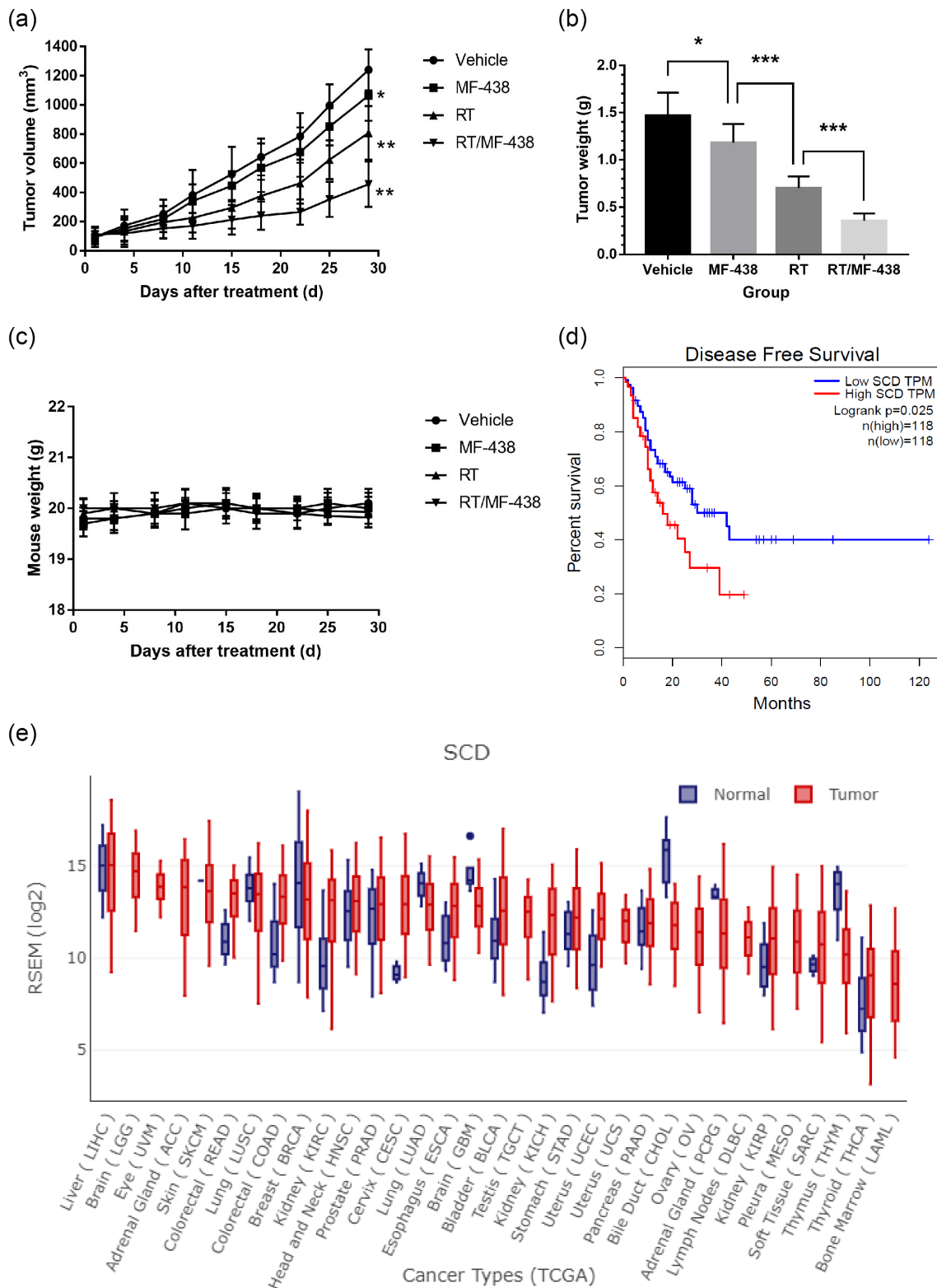


Figure 6. SCD1 inhibitor (MF-438), RT, or the combination of RT and MF-438 attenuated ESCC growth in vivo. (a) Treatment with MF-438, RT, or RT/MF-438 decreased the tumor volume compared with vehicle treatment. (b) Tumor weight was decreased after MF-438, RT, or RT/MF-438 compared with vehicle (c) MF-438 treatment had limited effect on mice body weight. (d) Low SCD expression (n = 118) is associated with favorable disease-free survival in ESCC patients. (e) SCD was overexpressed in cancer tissues compared with normal epithelium in esophagus. Data are expressed as means \pm SD (n = 5), p > .05; *p < 0.05; **p < 0.01; ***p < 0.001; ****p < 0.0001. **Abbreviations:** ESCC, esophageal squamous cell carcinoma; RT, radiation therapy; SCD, stearyl-coa desaturase; n.s, non-significant.

ferroptosis.^{18,26} However, ferroptotic cell death could not be mitigated with exogenous saturated fatty acids, indirectly emphasizing the crucial role of SCD1 in regulating ferroptosis.²⁶ Consistent with these analyses, in the current study, we observed that blockade of SCD1 with small molecular compound MF-438 was able to trigger lipid peroxidation. Furthermore, intracellular lipid peroxidation could be attenuated by supplementation of OA and POA.

It was not until relatively recently that the role of RT in mediating cancer cell ferroptosis had started being investigated and analyzed.^{9,13} Lei et al. reported that RT was capable of inducing the production of reactive oxygen species and high expression of ACSL4, resulting in accumulation of lipid peroxidation and tumor cell ferroptosis.¹⁴ Similarly, RT-induced lipid peroxidation biosynthesis was detected in the present analysis. MF-438 was effective in inhibiting the production of POA and OA, resulted in impaired lipid metabolism; the combination of RT and MF-438 caused a great amount of intracellular lipid peroxidation accumulation. Immediately, cancer cell membrane structures were destroyed and it resulted in ferroptotic cell death. On the other hand, radiation-induced lipid peroxidation could be alleviated by treatment with exogenous monounsaturated fatty acids, resulting in protection from ferroptosis (Figure 7).

With respect to RT, there have been several studies focused on ferroptosis and radiation resistance. High expression of SCL7A11 has been described to promote radiation resistance

by decreasing ferroptosis in ESCC.¹⁵ Indeed, SLC7A11 and GPX4 have been shown to be upregulated as an adaptive response to RT, thereby alleviating ferroptosis in tumor cells.¹⁴ p53 deficiency conferred radiation resistance via upregulating SLC7A11 expression and suppressing glutathione synthesis, resulting in decreased lipid peroxidation in tumor cells.³⁷ Nevertheless, another study found that RT-derived IFN γ activated ATM kinase and immunotherapy-activated CD8 + T cells were able to promote ferroptosis by inhibiting SLC7A11.³⁸ Given the complicated nature of lipid metabolism, it is not surprising to find conflicting reports. The current study confirmed that stimulating ferroptotic cell death was associated with enhanced efficacy of RT by using RSL3, whereas Fer-1 alleviated the radiation sensitivity of ESCC cells by attenuating ferroptosis. Additionally, our analyses indicated that SCD1 was involved in radiation resistance by regulating lipid metabolism and SCD1 inhibitors have been recognized as novel radio-sensitizers by suppressing lipid metabolism. This provides a novel target for new and innovative approaches in radiation sensitization.

Emerging evidence have implicated ferroptosis in activation of antitumor immunity.^{25,39} During the early stage of ferroptosis, cancer cells have been shown to release damage-associated molecular patterns (DAMPs), stimulating immunogenicity.²⁴ In our study, we explored the immunogenicity of ferroptotic tumor cells. We found that ferroptotic tumor cells assisted the activation of DCs; suppressing SCD1 or GPX4 enhanced radiation-mediated immunogenic ferroptosis, representing a novel ICD

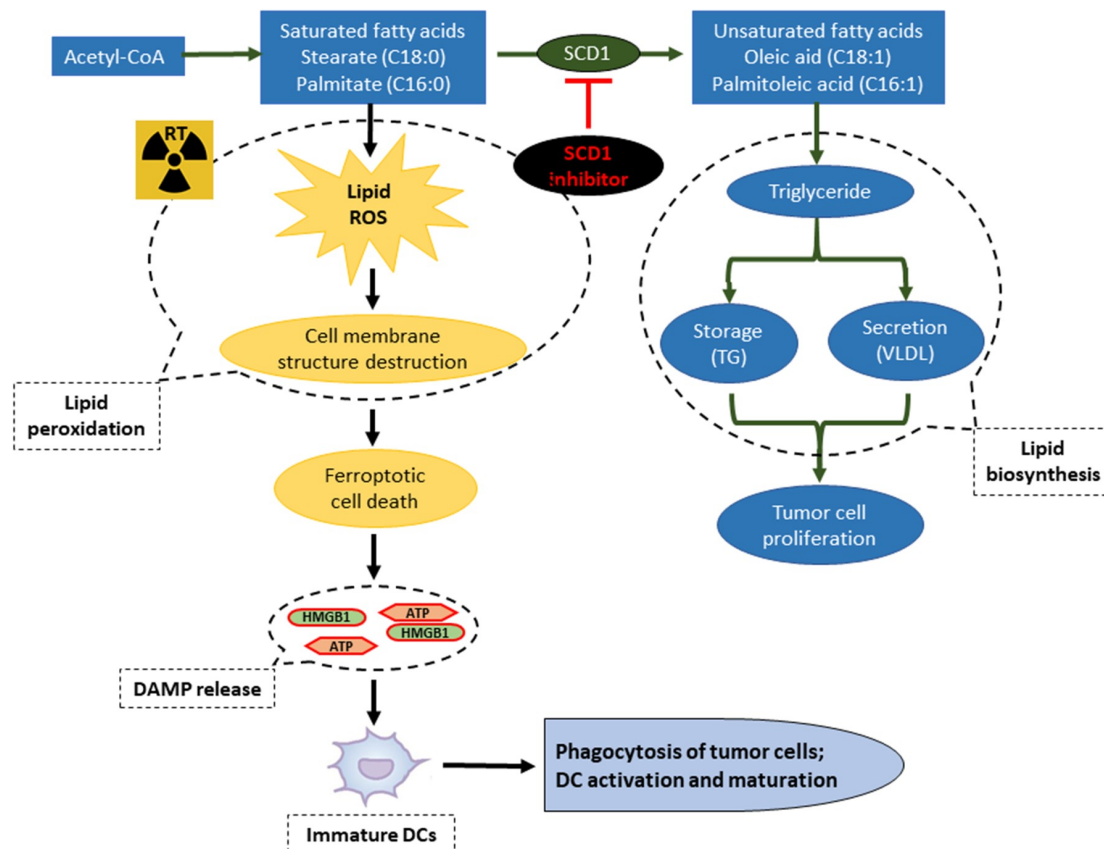


Figure 7. Proposed mechanism of MF-438-associated boost RT efficacy in human ESCC cell lines with high SCD1 expression by induction of immunogenic ferroptosis. **Abbreviations:** ATP, adenosine triphosphate; DAMP, damage-associated molecular patterns; DC, dendric cell; ESCC, esophageal squamous cell carcinoma; HMGB1, High mobility group box protein 1; ROS, reactive oxygen species; RT, radiation therapy; SCD1, stearyl-coa desaturase.

inducer. Although induction of ferroptosis was less efficient in stimulating calreticulin translocation to the membrane, RT was able to stimulate it efficiently, and further investigation is needed to clarify whether membrane calreticulin was expressed in early ferroptotic cancer cells. These findings present strong evidence of a novel strategy to improve the efficacy of RT.

Since difficulty swallowing and unintended weight loss were the most common symptoms of esophageal cancer, iron deficiency anemia may exist in the affected individuals.⁴⁰ Besides, tumor cells themselves exhibit an increased iron uptake to support survival.⁴¹ Anemia was an unfavorable factor with regards to treatment response and survival in cancer patients.⁶ In a mouse glioma model, administration of iron-containing water prior to RT stimulated ferroptotic cell death and decreased tumor size. Moreover, there was significant difference in tumor volume between mice treated with RT alone and mice treated with RT followed by the iron-containing water.^{42,43} Tumor cells containing high iron levels caused increased hydrogen peroxide generation, an early and crucial step for ferroptosis.⁴⁴ In addition, lactoferrin was an iron-binding multifunctional cationic glycoprotein that capable of treating iron deficiency anemia.⁴⁵ Holo-lactoferrin – a protein incorporated in food supplements to increase iron levels – exhibited anticancer properties via reactive oxygen species generation and GPX4 downregulation, resulting in tumor cell ferroptosis and enhanced radiation response in triple-negative breast cancer.⁴⁶ Consequently, the efficacy of RT combined with MF-438 may be improved with an increased cellular iron, especially in gastrointestinal tract tumors, and further study is warranted.

Emerging data from recent investigations identified several ferroptosis-based prognostic and therapeutic biomarkers in cancer.⁴⁷ SLC7A11 is an essential ferroptosis regulator that associated with poor outcomes in ESCC patients treated with RT.¹⁵ The ferroptosis-associated long non-coding RNAs signatures can be considered accurate and stable predictors of radiation response and survival outcomes in glioma.⁴⁸ Our analysis addressed SCD1 as an attractive target and a poor prognostic indicator of ESCC, this can contribute to future patient stratification and individualized treatment. Regardless, abnormal overexpression of SCD1 in ESCC cells should to be examined further.

In summary, our findings established that SCD1 protects ESCC cells from ferroptosis by mediating OA and POA synthesis, which promote radiation resistance. Targeting SCD1 with new drugs is a promising strategy that safely boosts RT. Overall, the essential role of lipid metabolism represents a novel therapeutic target to trigger immunogenic ferroptosis in cancer cells.

Data availability statement

The authors confirm that the data supporting the findings of this study are available within the article and its supplementary materials.

Disclosure statement

No potential conflict of interest was reported by the author(s).

Funding

This work was supported by The National Natural Science Foundation of China [no. 81773230]; The Science and Technology Research Plan of Henan [no. 212102310619]; The Medical Science and Technology Research Program of Henan [no. LHGJ20210171] and Bethune Cancer Radiotherapy Translational Medicine Research Program [no. flzh202115].

ORCID

Hong Ge  <http://orcid.org/0000-0003-4270-2556>

References

1. Lin DC, Wang MR, Koeffler HP. Genomic and epigenomic aberrations in esophageal squamous cell carcinoma and implications for patients. *Gastroenterology*. 2018;154(2):374–389. doi:10.1053/j.gastro.2017.06.066
2. Siegel RL, Miller KD, Fuchs HE, Jemal A. Cancer statistics, 2021. *CA Cancer J Clin*. 2021;71(1):7–33. doi:10.3322/caac.21654
3. Abnet CC, Arnold M, Wei W-Q. Epidemiology of esophageal squamous cell carcinoma. *Gastroenterology*. 2018;154(2):360–373. doi:10.1053/j.gastro.2017.08.023
4. Luo H, Ge H. Hot tea consumption and esophageal cancer risk: a meta-analysis of observational studies. *Front Nutr*. 2022;9:831567. doi:10.3389/fnut.2022.831567
5. Pucci C, Martinelli C, Ciofani G. Innovative approaches for cancer treatment: current perspectives and new challenges. *Ecancermedicalscience*. 2019;13:961. doi:10.3332/ecancer.2019.961
6. Natalucci V, Virgili E, Calcagnoli F, Valli G, Agostini D, Zeppa SD, Barbieri E, Emili R, Bai J, Zhang B. Cancer related anemia: an integrated multitarget approach and lifestyle interventions. *Nutrients*. 2021;14(1):13. doi:10.3390/nu14010013
7. Yang H, Liu H, Chen Y, Zhu C, Fang W, Yu Z, Mao W, Xiang J, Han Y, Chen Z, et al. Long-term efficacy of neoadjuvant chemoradiotherapy plus surgery for the treatment of locally advanced esophageal squamous cell carcinoma: the NEOCRTEC5010 randomized clinical trial. *JAMA Surg*. 2021;156(8):721–729. doi:10.1001/jamasurg.2021.2373
8. Bolm L, Kasmann L, Paysen A, Karapetis C, Rades D, Wellner UF, Keck T, Watson DI, Hummel R, Hussey DJ. Multimodal anti-tumor approaches combined with immunotherapy to overcome tumor resistance in esophageal and gastric cancer. *Anticancer Res*. 2018;38(6):3231–3242. doi:10.21873/anticancer.12588
9. Jiang X, Stockwell BR, Conrad M. Ferroptosis: mechanisms, biology and role in disease. *Nat Rev Mol Cell Biol*. 2021;22(4):266–282. doi:10.1038/s41580-020-00324-8
10. Chen X, Kang R, Kroemer G, Tang D. Broadening horizons: the role of ferroptosis in cancer. *Nat Rev Clin Oncol*. 2021;18(5):280–296. doi:10.1038/s41571-020-00462-0
11. Sia J, Szymd R, Hau E, Gee HE. Molecular mechanisms of radiation-induced cancer cell death: a primer. *Front Cell Dev Biol*. 2020;8:41. doi:10.3389/fcell.2020.00041
12. Zhang X, Xing X, Liu H, Feng J, Tian M, Chang S, Liu P, Zhang H. Ionizing radiation induces ferroptosis in granulocyte-macrophage hematopoietic progenitor cells of murine bone marrow. *Int J Radiat Biol*. 2020;96(5):584–595. doi:10.1080/09553002.2020.1708993
13. Yuan ZH, Liu T, Wang H, Xue LX, Wang JJ. Fatty acids metabolism: the bridge between ferroptosis and ionizing radiation. *Front Cell Dev Biol*. 2021;9:675617. doi:10.3389/fcell.2021.675617
14. Lei G, Zhang Y, Koppula P, Liu X, Zhang J, Lin SH, Ajani JA, Xiao Q, Liao Z, Wang H, et al. The role of ferroptosis in ionizing radiation-induced cell death and tumor suppression. *Cell Res*. 2020;30(2):146–162. doi:10.1038/s41422-019-0263-3
15. Feng L, Zhao K, Sun L, Yin X, Zhang J, Liu C, Li B. SLC7A11 regulated by NRF2 modulates esophageal squamous cell carcinoma radiosensitivity by inhibiting ferroptosis. *J Transl Med*. 2021;19(1):367. doi:10.1186/s12967-021-03042-7

16. Ye LF, Chaudhary KR, Zandkarimi F, Harken AD, Kinslow CJ, Upadhyayula PS, Dovas A, Higgins DM, Tan H, Zhang Y, et al. Radiation-induced lipid peroxidation triggers ferroptosis and synergizes with ferroptosis inducers. *ACS Chem Biol.* 2020;15(2):469–484. doi:10.1021/acscchembio.9b00939
17. Li D, Li Y. The interaction between ferroptosis and lipid metabolism in cancer. *Signal Transduct Target Ther.* 2020;5(1):108. doi:10.1038/s41392-020-00216-5
18. Ubellacker JM, Tasdogan A, Ramesh V, Shen B, Mitchell EC, Martin-Sandoval MS, Gu Z, McCormick ML, Durham AB, Spitz DR, et al. Lymph protects metastasizing melanoma cells from ferroptosis. *Nature.* 2020;585(7823):113–118. doi:10.1038/s41586-020-2623-z
19. Folwaczny A, Waldmann E, Altenhofer J, Henze K, Parhofer KG, Huang F, Jia X, Li L, Bai J, Zhang B. Postprandial lipid metabolism in normolipidemic subjects and patients with mild to moderate hypertriglyceridemia: effects of test meals containing saturated fatty acids, mono-unsaturated fatty acids, or medium-chain fatty acids. *Nutrients.* 2021;14:13.
20. Poloni S, Blom HJ, Schwartz V. Stearoyl-CoA desaturase-1: is it the link between sulfur amino acids and lipid metabolism? *Biology.* 2015;4(2):383–396. doi:10.3390/biology4020383
21. Khan W, Augustine D, Rao RS, Patil S, Awan KH, Sowmya SV, Haragannavar VC, Prasad K. Lipid metabolism in cancer: a systematic review. *J Carcinog.* 2021;20(1):4. doi:10.4103/jcar.JCar_15_20
22. Miess H, Dankworth B, Gouw AM, Rosenfeldt M, Schmitz W, Jiang M, Saunders B, Howell M, Downward J, Felsner DW, et al. The glutathione redox system is essential to prevent ferroptosis caused by impaired lipid metabolism in clear cell renal cell carcinoma. *Oncogene.* 2018;37(40):5435–5450. doi:10.1038/s41388-018-0315-z
23. Oatman N, Dasgupta N, Arora P, Choi K, Gawali MV, Gupta N, Parameswaran S, Salomone J, Reisz JA, Lawler S, et al. Mechanisms of stearoyl CoA desaturase inhibitor sensitivity and acquired resistance in cancer. *Sci Adv.* 2021;7(7). doi:10.1126/sciadv.abd7459
24. Efimova I, Catanzaro E, Van der Meeren L, Turubanova VD, Hammad H, Mishchenko TA, Vedunova MV, Fimognari C, Bachert C, Coppieters F, et al. Vaccination with early ferroptotic cancer cells induces efficient antitumor immunity. *J Immunother Cancer.* 2020;2:8.
25. Tang D, Kepp O, Kroemer G. Ferroptosis becomes immunogenic: implications for anticancer treatments. *Oncoimmunology.* 2020;10(1):1862949. doi:10.1080/2162402X.2020.1862949
26. Tesfay L, Paul BT, Konstorum A, Deng Z, Cox AO, Lee J, Furdui CM, Hegde P, Torti FM, Torti SV. Stearoyl-CoA desaturase 1 protects ovarian cancer cells from ferroptotic cell death. *Cancer Res.* 2019;79(20):5355–5366. doi:10.1158/0008-5472.CAN-19-0369
27. Luo H, Wang X, Wang Y, Dan Q, Ge H. Mannose enhances the radio-sensitivity of esophageal squamous cell carcinoma with low MPI expression by suppressing glycolysis. *Discover Oncol.* 2022;13(1):1. doi:10.1007/s12672-021-00447-0
28. Magtanong L, Ko PJ, To M, Cao JY, Forcina GC, Tarangelo A, Ward CC, Cho K, Patti GJ, Nomura DK, et al. Exogenous mono-unsaturated fatty acids promote a ferroptosis-resistant cell state. *Cell Chem Biol.* 2019;26:420–32 e9.
29. Kroemer G, Galluzzi L, Kepp O, Zitvogel L. Immunogenic cell death in cancer therapy. *Annu Rev Immunol.* 2013;31(1):51–72. doi:10.1146/annurev-immunol-032712-100008
30. Galluzzi L, Vitale I, Warren S, Adjemian S, Agostinis P, Martinez AB, Chan TA, Coukos G, Demaria S, and Deutsch E, et al. Consensus guidelines for the definition, detection and interpretation of immunogenic cell death. *J Immunother Cancer.* 2020;8(1): e000337. doi:10.1136/jitc-2019-000337.
31. Galluzzi L, Kepp O, Kroemer G. Immunogenic cell death in radiation therapy. *Oncoimmunology.* 2013;2(10):e26536. doi:10.4161/onci.26536
32. Golden EB, Frances D, Pellicciotta I, Demaria S, Helen Barcellos-Hoff M, Formenti SC. Radiation fosters dose-dependent and chemotherapy-induced immunogenic cell death. *Oncoimmunology.* 2014;3(4):e28518. doi:10.4161/onci.28518
33. Yang WS, Kim KJ, Gaschler MM, Patel M, Shchepinov MS, Stockwell BR. Peroxidation of polyunsaturated fatty acids by lipoxygenases drives ferroptosis. *Proc Natl Acad Sci U S A.* 2016;113(34):E4966–75. doi:10.1073/pnas.1603244113
34. Doll S, Proneth B, Tyurina YY, Panzilius E, Kobayashi S, Ingold I, Irmeler M, Beckers J, Aichler M, Walch A, et al. ACSL4 dictates ferroptosis sensitivity by shaping cellular lipid composition. *Nat Chem Biol.* 2017;13(1):91–98. doi:10.1038/nchembio.2239
35. Kagan VE, Mao G, Qu F, Angeli JP, Doll S, Croix CS, Dar HH, Liu B, Tyurin VA, Ritov VB, et al. Oxidized arachidonic and adrenic PEs navigate cells to ferroptosis. *Nat Chem Biol.* 2017;13(1):81–90. doi:10.1038/nchembio.2238
36. Agmon E, Stockwell BR. Lipid homeostasis and regulated cell death. *Curr Opin Chem Biol.* 2017;39:83–89. doi:10.1016/j.cbpa.2017.06.002
37. Lei G, Zhang Y, Hong T, Zhang X, Liu X, Mao C, Yan Y, Koppula P, Cheng W, Sood AK, et al. Ferroptosis as a mechanism to mediate p53 function in tumor radiosensitivity. *Oncogene.* 2021;40(20):3533–3547. doi:10.1038/s41388-021-01790-w
38. Lang X, Green MD, Wang W, Yu J, Choi JE, Jiang L, Liao P, Zhou J, Zhang Q, Dow A, et al. Radiotherapy and immunotherapy promote tumoral lipid oxidation and ferroptosis via synergistic repression of SLC7A11. *Cancer Discov.* 2019;9(12):1673–1685. doi:10.1158/2159-8290.CD-19-0338
39. Demuyneck R, Efimova I, Naessens F, Krysko DV. Immunogenic ferroptosis and where to find it? *J Immunother Cancer.* 2021;9(12): e003430. doi:10.1136/jitc-2021-003430
40. Ludwig H, Muldur E, Endler G, Hubl W. Prevalence of iron deficiency across different tumors and its association with poor performance status, disease status and anemia. *Ann Oncol.* 2013;24(7):1886–1892. doi:10.1093/annonc/mdt118
41. Xia X, Fan X, Zhao M, Zhu P. The relationship between ferroptosis and tumors: a novel landscape for therapeutic approach. *Curr Gene Ther.* 2019;19(2):117–124. doi:10.2174/1566523219666190628152137
42. Ivanov SD, Semenov AL, Kovan'ko EG, Yamshanov VA. Effects of iron ions and iron chelation on the efficiency of experimental radiotherapy of animals with gliomas. *Bull Exp Biol Med.* 2015;158(6):800–803. doi:10.1007/s10517-015-2865-1
43. Ivanov SD, Semenov AL, Mikhelson VM, Kovan'ko EG, Yamshanov VA. Effects of iron ion additional introduction in radiation therapy of tumor-bearing animals. *Radiats Biol Radioecol.* 2013;53(3):296–303. doi:10.7868/s0869803113030065
44. Takashi Y, Tomita K, Kuwahara Y, Roudkenar MH, Roushbandeh AM, Igarashi K, Nagasawa T, Nishitani Y, Sato T. Mitochondrial dysfunction promotes aquaporin expression that controls hydrogen peroxide permeability and ferroptosis. *Free Radic Biol Med.* 2020;161:60–70. doi:10.1016/j.freeradbiomed.2020.09.027
45. Omar OM, Assem H, Ahmed D, Abd Elmaksoud MS. Lactoferrin versus iron hydroxide polymaltose complex for the treatment of iron deficiency anemia in children with cerebral palsy: a randomized controlled trial. *Eur J Pediatr.* 2021;180(8):2609–2618. doi:10.1007/s00431-021-04125-9
46. Zhang Z, Lu M, Chen C, Tong X, Li Y, Yang K, Lv H, Xu J, Qin L. Holo-lactoferrin: the link between ferroptosis and radiotherapy in triple-negative breast cancer. *Theranostics.* 2021;11(7):3167–3182. doi:10.7150/thno.52028
47. Wang H, Lin D, Yu Q, Li Z, Lenahan C, Dong Y, Wei Q, Shao A. A promising future of ferroptosis in tumor therapy. *Front Cell Dev Biol.* 2021;9:629150. doi:10.3389/fcell.2021.629150
48. Zheng J, Zhou Z, Qiu Y, Wang M, Yu H, Wu Z, Wang X, Jiang X. A prognostic ferroptosis-related lncRNAs signature associated with immune landscape and radiotherapy response in glioma. *Front Cell Dev Biol.* 2021;9:675555. doi:10.3389/fcell.2021.675555